ELSEVIER

Journal of Hazardous Materials B139 (2007) 122–131

Journal of Hazardous Materials

www.elsevier.com/locate/jhazmat

Removal of cadmium from aqueous solutions by adsorption onto orange waste

A.B. Pérez-Marín, V. Meseguer Zapata *, J.F. Ortuño, M. Aguilar, J. Sáez, M. Lloréns

Department of Chemical Engineering, University of Murcia, 30071 Murcia, Spain

Received 26 July 2005; received in revised form 24 April 2006; accepted 6 June 2006
Available online 10 June 2006

Abstract

The use of orange wastes, generated in the orange juice industry, for removing cadmium from aqueous solutions has been investigated. The material was characterized by Fourier transform infrared spectroscopy and batch experiments were conducted to determine the adsorption capacity of the biomass. A strong dependence of the adsorption capacity on pH was observed, the capacity increasing as pH value rose. Kinetics and adsorption equilibrium were studied at different pH values (4–6). The adsorption process was quick and the equilibrium was attained within 3 h. The maximum adsorption capacity of orange waste was found to be 0.40, 0.41 and 0.43 mmol/g at pH 4–6, respectively. The kinetic data were analysed using various kinetic models – pseudo-first order equation, pseudo-second order equation, Elovich equation and intraparticle diffusion equation – and the equilibrium data were tested using four isotherm models – Langmuir, Freundlich, Sips and Redlich–Peterson. The data were fitted by non-linear regression and five error analysis methods were used to evaluate the goodness of the fit. The Elovich equation provides the greatest accuracy for the kinetic data and the Sips model the closest fit for the equilibrium data.

Keywords: Adsorption; Isothermal; Kinetics; Cadmium; Orange waste

1. Introduction

The increase in environmental pollution caused by toxic metals is of great concern because of their carcinogenic properties [1], their non-biodegradability and bio-accumulation.

Cadmium may be found in wastewater discharges from the electroplating industry, the manufacture of nickel–cadmium batteries, fertilizers, pesticides, pigments and dyes and textile operations [2,3]. It is non-biodegradable and travels through the food chain. In humans, nausea and vomiting has been recorded at levels of 15 mg Cd^{2+}/l with no adverse effects at 0.05 mg Cd^{2+}/l. Severe toxic, but non fatal, symptoms are reported at concentrations of 10–326 mg Cd^{2+}/l of cadmium. The kidneys are the critical target organ after ingestion (renal dysfunction, hypertension and anaemia) [4,5].

Hence, there is great interest regarding the removal of cadmium from wastewater streams. Conventional methods for heavy metal removal from wastewater include reduction, precipitation, ion exchange, filtration, electrochemical treatment, membrane technology and evaporation removal, all of which may be ineffective or extremely expensive, when the metals are dissolved in large volumes of solution at relatively low concentrations [6,7].

In this setting, the use of low-cost materials (industrial, agricultural or urban residues) for recovering heavy metals from contaminated industrial effluent has emerged as a potential alternative method to conventional techniques. For example, some of the non-conventional low cost adsorbents recently used for the removal of heavy metals are hazelnut shell, apple residues, banana pith, tree leaves, mandarin peels, rice polish, seeds of *Capsicum annuum* and *Ceiba pentandra* hulls [8–15].

The aim of the present study was to explore the feasibility of using orange residues proceeding from the orange juice and soft-drinks industries as an adsorbent for the removal of cadmium. Orange waste contains cellulose, pectins, hemicellulose, chlorophyll pigments and other low molecular weight compounds, including limonene. Some authors have described the functional carboxylic groups of the pectins and the alcoholic

* Corresponding author. Tel.: +34 968 36 75 15; fax: +34 968 36 41 48.
E-mail address: vzapata@um.es (V.M. Zapata).

0304-3894/$ – see front matter © 2006 Elsevier B.V. All rights reserved.
doi:10.1016/j.jhazmat.2006.06.008

hydroxyl groups of the celluloses as the active binding sites for metals [16].

The effect of pH on cadmium adsorption, kinetics and adsorption equilibrium were investigated. Both, the kinetic and adsorption isotherms were analysed by non-linear regression using different models. In order to determine the best fit for each system, five error analysis methods were used to evaluate the data.

Non-linear optimisation is advisable. Transformation of non-linear equations to linear forms implicitly alters their error structure and may also violate the error variance and normality assumptions of standard least squares [17].

2. Materials and methods

2.1. Adsorbent

The orange waste used as adsorbent in this study was obtained from the orange juice industry. The orange waste was first cut into small pieces, was extensively washed with tap water to remove adhering dirt and soluble components such as tannins, resins, reducing sugar and colouring agents, and then was oven-dried at 50–60 °C until constant weight. The washed and dried material was crushed and sieved to obtain a particle size lower than 1.5 mm. Biomass was characterized by Fourier transform infrared spectroscopy (FTIR) (Perkin-Elmer 16F PC).

2.2. Chemical

Stock cadmium solution (2000 mg/l, 17.8 mM) was prepared by dissolving 2 g of analytical grade cadmium metal supplied by Merck in a mixture of 50 ml of distilled water and 10 ml of concentrated nitric acid, and diluting to a litre with distilled water. This stock solution was then diluted to specified concentrations. All chemicals were used of analytical reagent grade and purchased from PANREAC.

2.3. Experimental procedure

Adsorption studies were carried out by batch process. Biomass was added to glass flasks containing a known amount of metal solution of the desired concentration. The mixture was stirred magnetically for 3 h, time more than sufficient to reach equilibrium. The pH of solutions was adjusted by adding dilute solutions of HNO_3 and NH_4OH. The biosolids were then removed by filtration through glass fibre prefilters (Milipore AP40) and the filtrates were analysed for residual cadmium concentration by atomic adsorption spectrophotometry (Perkin-Elmer model AA300) with an air–acetylene flame. Cadmium hollow cathode lamp was used. The spectral slit width and the working wavelength were 0.7 and 228.8 nm, respectively. Atomic absorption standard solutions (PANREAC) were used.

Metal uptake (q, mmol/g) was calculated using the general definition:

$$q = \frac{C_0 V_0 - C_f V_f}{m} \quad (1)$$

where C_0 and C_f are the initial and final metal concentrations in solution (mmol/l), respectively, V_0 and V_f are the initial and final solution volumes (l), respectively and m is the mass of the biosorbent used (g).

All experiments were performed in duplicate at least and mean values were presented with a maximum deviation of 5% in all the cases studied.

Blank samples were run under similar experimental conditions but in the absence of adsorbent. It was not detected chemical precipitation and losses of cadmium to the containers wall.

2.3.1. Preliminary experiments

Batch experiments were performed to determine the effect of various parameters (adsorbent dosage and the particle size) on the sorption of Cd^{2+} onto orange waste.

In order to study the dependence of Cd^{2+} sorption on particle size, experiments were carried out with different particle size fraction (<0.3, 0.3–0.5, 0.5–0.8, 0.8–1, 1–1.25, 1.25–1.5, 1.5–2.5 mm). A 0.2 g of biomass was added to glass flasks containing 50 ml of metal solution (100 mg/l). The mixture was stirred magnetically for a contact time of 3 h, at room temperature and at pH 4.

The effect of adsorbent dosage on sorption of Cd^{2+} was obtained by agitating 50 ml of metal solution (100 mg/l) with 0.0125, 0.025, 0.05, 0.075, 0.1, 0.15, 0.2, 0.25, 0.3 and 0.4 g of adsorbent for 3 h at room temperature and at constant pH (pH 4).

2.3.2. Effect of pH

Batch experiments were carried out by taking in contact 50 ml of cadmium solution (100 mg/l) with 0.2 g of biomass for 3 h adjusting continuously the solution pH at several pH values (2–6).

2.3.3. Kinetic of adsorption

Kinetic studies were carried out in a glass beaker with magnetic stirring at room temperature (25 °C). Four grams of biomass was added to 1 l of cadmium solution (100 mg/l) and the pH of the solution was maintained constant throughout the experiment. Kinetic studies were carried out at pH 4–6. Samples were taken at predetermined time intervals using 20 cm^3 syringes and filtered immediately through glass fibre prefilters and the filtrate was analyzed to determine the cadmium remaining.

2.3.4. Adsorption isotherm

A 0.2 g of biomass was added to glass flasks containing 50 ml of metal solution. The cadmium concentration was varied in the range of 15–500 mg/l, for a contact time of 3 h. Adsorption isotherms were obtained at pH 4–6.

3. Theory

3.1. Kinetic model

The adsorption kinetic shows the evolution of the adsorption capacity with time. To examine the potential rate-controlling

step (e.g. chemical reaction, diffusion control and mass transfer), several kinetic models were used to test the experimental data [3,18–21].

3.1.1. Pseudo-first order equation

The pseudo-first order equation is generally expressed as follows:

$$\frac{dq_t}{dt} = k_1(q_e - q_t) \quad (2)$$

where q_e and q_t (mmol/g) are the amount of cadmium sorbed at equilibrium and at time t (min), respectively, and k_1 (min^{-1}) is the rate constant of the pseudo-first order equation.

After integration and applying the boundary conditions, for $q_t = 0$ at $t = 0$ and $q_t = q_t$ at $t = t$, the equation becomes:

$$q_t = q_e(1 - e^{-k_1 t}) \quad (3)$$

3.1.2. Pseudo-second order equation

The pseudo-second order equation is expressed as:

$$\frac{dq_t}{dt} = k_2(q_e - q_t)^2 \quad (4)$$

Integrating this equation for the boundary conditions, gives:

$$q_t = \frac{t}{(1/k_2 q_e{}^2) + (t/q_e)} \quad (5)$$

where k_2 is the equilibrium rate constant of the pseudo-second order equation (g/mmol min) and $k_2 q_e{}^2 = h$ is the initial adsorption rate (mmol/g min).

3.1.3. The Elovich equation

The Elovich equation is of general application to chemisorption kinetics. The equation has been applied satisfactorily to some chemisorption processes and has been found to cover a wide range of slow adsorption rates. The same equation is often valid for systems in which the adsorbing surface is heterogeneous, and is formulated as:

$$\frac{dq_t}{dt} = \alpha e^{-\beta q_t} \quad (6)$$

Integrating this equation for the boundary conditions, gives:

$$q_t = \frac{1}{\beta}\ln(\alpha\beta) + \frac{1}{\beta}\ln t \quad (7)$$

where α (mmol/g min) is the initial adsorption rate and β is related to the extent of surface coverage and the activation energy involved in chemisorption (g/mmol).

3.1.4. Intraparticle diffusion equation

The intraparticle diffusion equation is given as:

$$q_t = k\sqrt{t} \quad (8)$$

where k (mmol/g min$^{1/2}$) is the intraparticle diffusion rate constant.

3.2. Equilibrium isotherm models

An adsorption isotherm describes the relationship between the amount of metal adsorbed and the metal ion concentration remaining in solution. There are many equations for analysing experimental adsorption equilibrium data. The equation parameters and the underlying thermodynamic assumptions of these equilibrium models often provide some insight into both the adsorption mechanism and the surface properties and affinity of the sorbent. In this work, the following four models were tested:

3.2.1. The Langmuir isotherm

The Langmuir isotherm is based on the following assumptions [22]:

- metals ions are chemically adsorbed at a fixed number of well-defined sites,
- each site can only hold one ion,
- all sites are energetically equivalent, and
- there is no interaction between the ions.

The Langmuir equation is formulated as [23]:

$$q_e = \frac{q_{max} b C_e}{1 + bC_e} \quad (9)$$

where C_e (mmol/l) and q_e (mmol/g) are the equilibrium concentrations in the liquid and solid phase, respectively, q_{max} is a Langmuir constant that expresses the maximum metal uptake (mmol/g) and b is also a Langmuir constant related to the energy of adsorption and affinity of the sorbent.

3.2.2. Freundlich isotherm

Freundlich expression is an exponential equation and therefore assumes that the concentration of adsorbate on the adsorbent surface increases with the adsorbate concentration. Theoretically, using this expression, an infinite amount of adsorption can occur [24]. The equation is widely applied in heterogeneous systems:

$$q_e = k_F C_e^{1/n} \quad (10)$$

where k_F (l/g) and n are Freundlich constants characteristic of the system, indicating the adsorption capacity and adsorption intensity, respectively.

3.2.3. Sips isotherm

The model is a combination of the Langmuir and Freundlich isotherm type models. The Sips model takes the following form [25]:

$$q_e = \frac{q_{max} b C_e^{1/n}}{1 + bC_e^{1/n}} \quad (11)$$

At low sorbate concentrations it effectively reduces to a Freundlich isotherm, while at high sorbate concentrations it predicts a monolayer adsorption capacity characteristic of the Langmuir isotherm.

3.2.4. Redlich–Peterson isotherm

Redlich and Peterson [26] proposed an empirical equation to represent equilibrium data:

$$q_e = \frac{k_R C_e}{1 + a_R C_e^{\beta}} \quad \text{where } \beta \leq 1 \tag{12}$$

where k_R (l/g), a_R (l/mmol) and β are Redlich–Peterson isotherm constants. This equation reduces to a linear isotherm in the case of low surface coverage and to a Langmuir isotherm when $\beta = 1$.

3.3. Determining equation parameters by non-linear regression

For the different kinetic models and equilibrium equations, parameter sets were determined by non-linear regression, which is a mathematically rigorous method that uses the original form of the equation [27].

Since the choice of error function can affect the parameters derived, five different error functions were examined and in each case the parameters were determined by minimising the respective error function using the Solver add-in with Microsoft spreadsheet, Excel.

The error functions employed were as follows:

- The sum of the square of the errors (ERRSQ):

$$\sum_{i=1}^{p} (q_{exp} - q_{cal})_i^2 \tag{13}$$

This widely used error function has one major drawback. Parameters derived using this error function will provide a better fit as the magnitude of the errors (and thus the squares of the errors) increase—biasing the fit towards data obtained at the high end of the concentration range.

- The hybrid fractional error function (HYBRID):

This error function was developed [28] in order to improve the fit of the ERRSQ method at low concentration values

$$\frac{100}{p-n} \sum_{i=1}^{p} \left[\frac{(q_{exp} - q_{cal})^2}{q_{exp}} \right]_i \tag{14}$$

where p is the number of data points and n the number of parameters within the equation.

- Marquardt's percent standard deviation (MPSD) [29]:

$$100 \left[\sqrt{\frac{1}{p-n} \sum_{i=1}^{p} \left(\frac{q_{exp} - q_{cal}}{q_{exp}} \right)_i^2} \right] \tag{15}$$

This is similar in some respects to a geometric mean error distribution modified according to the number of degrees of freedom of the system.

- The average relative error (ARE) [30], which minimises the fractional error distribution across the entire concentration range.

$$\frac{100}{p} \sum_{i=1}^{p} \left(\frac{|q_{exp} - q_{cal}|}{q_{exp}} \right)_i \tag{16}$$

- The sum of the absolute errors (EABS), which is similar to the sum of the squares of the errors.

$$\sum_{i=1}^{p} |q_{exp} - q_{cal}|_i \tag{17}$$

Each error criterion provides a different set of parameters. Hence, in order to compare between the parameter sets, a procedure for normalising and combining the error results was adopted to obtain the so-called 'sum of the normalised error (SNE)' for each parameter set of each equation. The SNE was calculated by determining the values of the error functions for each parameter set, dividing the errors determined for a given error function by the maximum for that error function to obtain the normalised error, and summing the normalised errors for each parameter set [28].

Using this method, the error function which provides the slowest SNE can be considered to give the closest fit.

4. Results and discussion

4.1. FTIR analysis

In order to determine which functional groups were responsible for metal uptake, an FTIR analysis in solid phase was performed on the biomass prepared in a KBr disk. FTIR spectra were obtained for adsorbent solid samples before and after the biosorption process [31–33]. As shown in Fig. 1, the spectra display a number of adsorption peaks, indicating the complex nature of the material examined.

The broad, intense absorption peaks around 3340 cm^{-1} are indicative of the existence of bounded hydroxyl groups (3340–3380 cm^{-1}). The peaks observed at 2924 cm^{-1} can be assigned to the C–H group. The peaks around 1647 cm^{-1} are due to the C=C stretching that can be attributed to the aromatic C–C bond, while the intense band at 1058 cm^{-1} can be assigned to the C–O of alcohols and carboxylic acids. All these peaks in the sample after adsorption show an absorbance substantially lower than those in the raw sample and small dif-

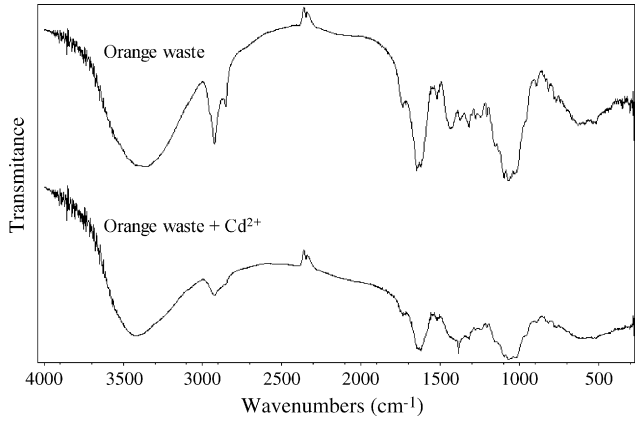

Fig. 1. FTIR spectra of the orange waste in BrK disk, before and after adsorption of Cd(II).

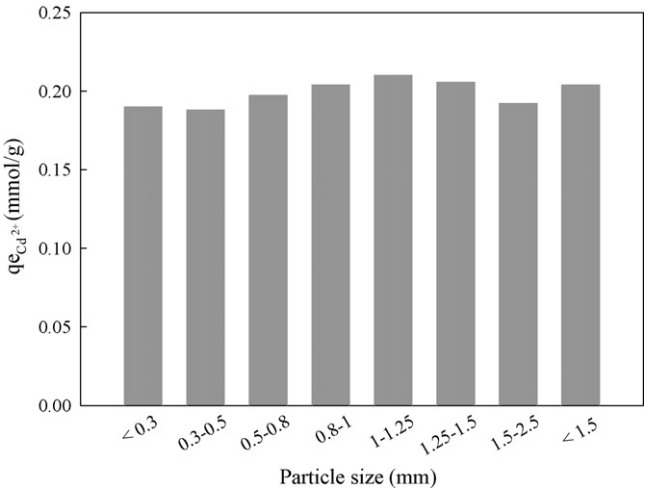

Fig. 2. Effect of particle size on cadmium removal.

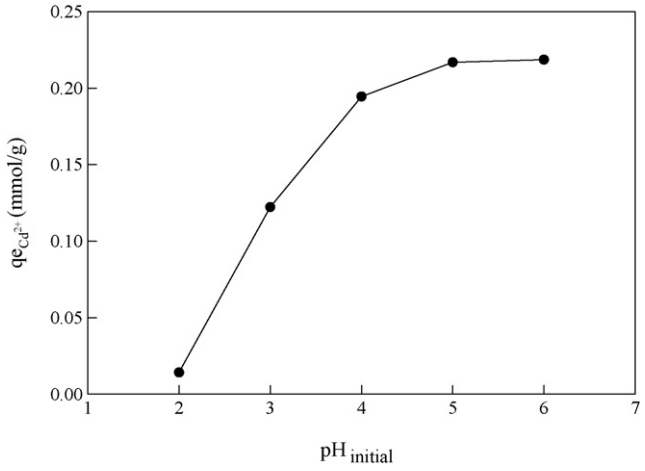

Fig. 4. Influence of the pH on sorption capacity onto orange waste.

ferences in the frequency bands, suggesting the participation of these functional groups in the adsorption of cadmium by orange waste.

4.2. Preliminary experiments

Variables of the system, including orange waste dose and particle size, were adopted to study their effects on Cd^{2+} removal.

The influence of particle size on cadmium removal is shown in Fig. 2. In the range studied, there were no significant differences in the Cd^{2+} sorption with varying particle size. The sorption capacity of orange waste with the different particle size fraction studied varies from 0.19 to 0.21 mmol/g. The sorption capacity of a global sample, <1.5 mm, was 0.2 mmol/g. Therefore, all the subsequent experiments were performed with this global sample.

The results of the experiments with varying adsorbent concentrations are presented in Fig. 3. Increasing the adsorbent concentration, up to 4 g/l dosage, resulted in a rapid increase in the percentage of cadmium uptake (0–80% cadmium uptake). A greater dosage leads to an increase in cadmium uptake significantly lower. For all the subsequent experiments an orange waste dosage of 4 g/l was selected.

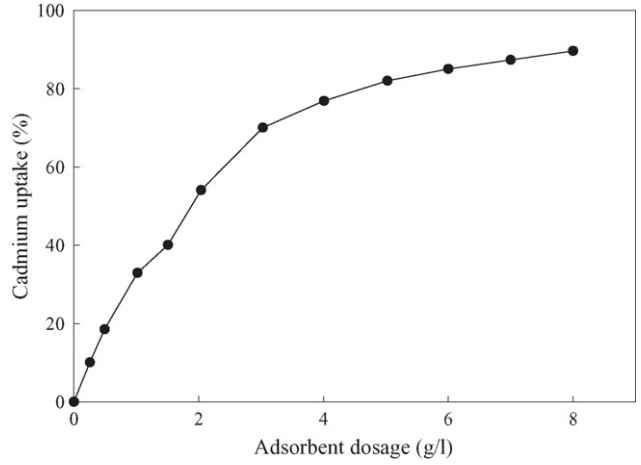

Fig. 3. Effect of orange waste dosage on cadmium removal.

4.3. Effect of pH

The pH of the aqueous solution is an important controlling parameter in the adsorption process [34–36]. Fig. 4 presents the effect of pH on the removal of cadmium in experiments carried out at different pH values. It can be seen that the adsorption capacity of cadmium(II) by orange waste is clearly affected by the pH, Cd uptake increasing with the pH. This dependence of metal uptake on pH may be related to the functional groups of the biomass and/or the solution chemistry [8,11].

At pH values below 8, cadmium is in its free ionic form (Cd^{2+}) [37,38] and, as such, the increase in metal uptake cannot be described by the change in metal speciation, which leads to the hypothesis that the cell wall functional groups and their associated ionic state are responsible for the extent of adsorption [31].

The minimal adsorption at low pH may be due to the higher concentration and high mobility of the H^+, which are preferentially adsorbed rather than the metal ions [11,35]. At higher pH values, the lower number of H^+ and greater number of ligands with negatives charges results in greater cadmium adsorption. For example, carboxylic groups (–COOH) are important groups for metal uptake by biological materials [33,39]. At pH higher than 3–4, carboxylic groups are deprotonated and negatively charged. Consequently, the attraction of positively charged metal ions would be enhanced [8].

4.4. Adsorption kinetics

The kinetic profiles of cadmium biosorption at various pH values are shown in Fig. 5. A very fast increase in the biosorption rate of cadmium to the orange waste may be observed in the 20 first minutes for all three pH values studied, followed by a less rapid increase and a practically constant plateau after 60 min, in all cases.

The rapid kinetics has significant practical importance, as it facilitates smaller reactor volumes, ensuring high efficiency and economy [20].

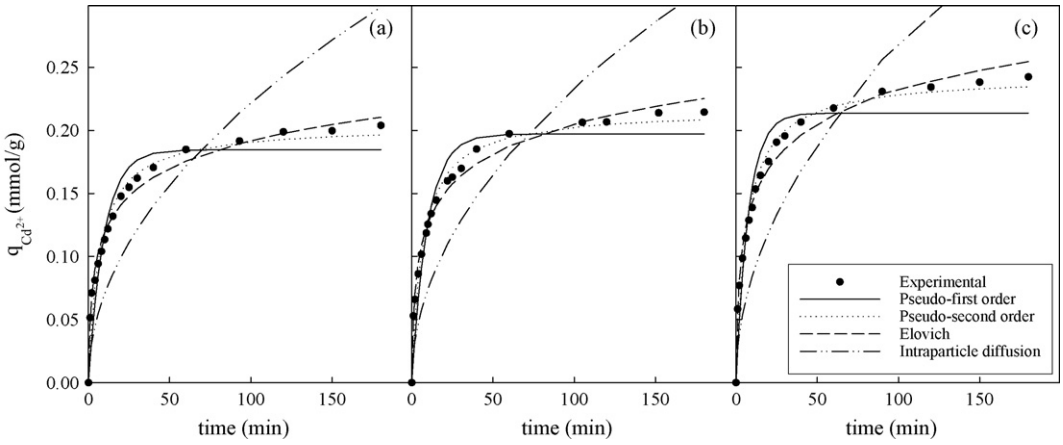

Fig. 5. Sorption kinetics of cadmium at (a) pH 4, (b) pH 5 and (c) pH 6.

In order to determine the potential rate-controlling step, several reaction-based and diffusion-based models were employed to test experimental data.

The experiments were performed in a well-stirred batch system, where all the binding sites were readily available for metal uptake, and hence the effect of external film diffusion cannot be considered as a limiting step. In addition, the relatively short contact time necessary to achieve equilibrium conditions is considered as an initial indication that the adsorption of cadmium is a chemical-reaction controlled, rather than diffusion controlled, process [17,20]. This was verified after adjusting experimental data to several mathematical models.

Four kinetic models – pseudo-first order equation, pseudo-second order equation, Elovich equation and intraparticle diffusion equation – were used to fit experimental data by non-linear regression, using five different error functions.

Fig. 5 shows the adsorption kinetics for cadmium on orange waste at several pH values and the fit to different kinetic models by non-linear regression, using the selected parameter sets. For 7 of the 12 cases studied (4 kinetic models × 3 pH values) the HYBRID parameter sets produced the best fit. ERRSQ produced the lowest SNE value for four of the remaining sets (Table 1). In order to interpret the parameter sets of the different models, the parameters giving the lowest SNE were used in each case. The pseudo-first order equation was used to correlate the experimental data, based on the following mechanistic scheme:

$$M_{sol} + Cd_{aq}{}^{2+} \rightarrow MCd_{solid\ phase}$$

One cadmium ion was assumed to sorb onto one adsorption site of the orange waste surface.

As can be seen in Fig. 5, pseudo-first order kinetic predicts a lower value of the equilibrium adsorption capacity than the experimental value. Hence, this equation cannot provide an accurate fit of the experimental data.

The pseudo-second order model assumes that cadmium is sorbed onto two active sites:

$$2M_{sol} + Cd_{aq}{}^{2+} \rightarrow M_2Cd_{solid\ phase}$$

Fig. 5 shows that the pseudo-second order equation provides a more accurate fit than pseudo-first order equation, giving lower values of the different error functions. Moreover, the equilibrium adsorption capacities, q_e, obtained with this model are slightly more reasonable than those of the pseudo-first order when comparing predicted results with experimental data. The initial adsorption rate, h, obtained for the pseudo-second order model increased with increasing pH values, while the values of the constant, k_2, decreased with increasing pH. This indicates that the contact time necessary to reach the equilibrium is affected by the pH values, more time being necessary to reach equilibrium with the higher values of pH.

The Elovich equation assumes that the active sites of the biosorbent are heterogeneous [5] and therefore exhibit different activation energies for chemisorption. Teng and Hsieh [40] proposed that constant α is related to the rate of chemisorption and β is related to the surface coverage. When the pH values increased, the constant α was observed to increase and the constant β to decrease (Table 1). Therefore, by increasing the pH value, within the range studied, the rate of chemisorption can be increased and the available adsorption surface for orange waste will decrease. This model provides the best fit to the experimental data, as can be seen for the different error values shown in Table 1. The previous successful applications of the Elovich equation to heterogeneous catalyst surfaces support its use for predicting the adsorption of cadmium onto orange wastes. In fact, it was shown in the FTIR analysis of the orange waste that this material presents a heterogeneous surface with different functional groups available to sorb cadmium. The Elovich equation is based on a general second-order reaction mechanism for heterogeneous adsorption processes [5].

The intraparticle equation did not provide a good fit to the experimental data (Fig. 5), and gave the highest error for all the studied cases. This fact confirms the earlier hypothesis that the adsorption process is controlled by chemical reaction.

4.5. Adsorption isotherm

Fig. 6 shows the experimental equilibrium data as well as the fit to the different isotherm models using the error criterion which provides the closest fit to the measured data.

Table 1
Kinetic constants with error analysis, at different pH values

	pH														
	4					5					6				
	ERRSQ	HYBRID	MPSD	ARE	EABS	ERRSQ	HYBRID	MPSD	ARE	EABS	ERRSQ	HYBRID	MPSD	ARE	EABS
Pseudo-first order equation															
q_e	0.186	0.179	0.164	0.185	0.190	0.197	0.189	0.175	0.187	0.198	0.222	0.214	0.199	0.208	0.218
k_1	0.099	0.123	0.178	0.104	0.086	0.103	0.128	0.179	0.112	0.101	0.106	0.129	0.1790	0.120	0.101
ERRSQ	0.005	0.005	0.009	0.005	0.005	0.005	0.005	0.008	0.005	0.005	0.005	0.006	0.0100	0.007	0.006
HYBRID	0.364	0.339	0.406	0.355	0.422	0.320	0.293	0.355	0.326	0.326	0.342	0.314	0.3807	0.346	0.375
MPSD	22.99	21.06	19.84	22.57	25.07	21.34	19.11	17.80	21.05	21.63	20.87	18.83	17.5669	20.15	22.00
ARE	13.11	13.44	14.83	13.02	13.61	12.09	12.37	13.67	12.05	12.08	11.97	11.99	13.2221	11.64	11.99
EABS	0.234	0.266	0.334	0.237	0.226	0.228	0.264	0.336	0.241	0.225	0.257	0.284	0.3582	0.267	0.247
SNE	3.91	3.95	4.75	**3.88**	4.18	**3.98**	4.01	4.82	4.11	4.00	4.00	**3.98**	4.79	4.10	4.15
Pseudo-second order equation															
q_e	0.204	0.196	0.182	0.208	0.211	0.216	0.209	0.198	0.217	0.217	0.243	0.236	0.2230	0.241	0.249
k_2	0.714	0.899	1.318	0.602	0.554	0.692	0.846	1.147	0.672	0.672	0.634	0.766	1.0328	0.625	0.539
h	0.030	0.035	0.044	0.026	0.025	0.032	0.037	0.045	0.032	0.032	0.038	0.043	0.0514	0.036	0.033
ERRSQ	0.002	0.002	0.004	0.002	0.002	0.001	0.002	0.003	0.001	0.001	0.002	0.002	0.0033	0.002	0.002
HYBRID	0.155	0.141	0.174	0.189	0.206	0.113	0.101	0.125	0.117	0.117	0.119	0.108	0.1337	0.123	0.151
MPSD	15.74	14.09	13.08	17.70	18.60	13.62	11.98	11.05	13.95	13.95	13.22	11.67	10.7566	13.70	15.10
ARE	7.73	8.33	9.98	7.50	7.71	6.42	6.97	8.20	6.37	6.37	6.28	6.61	7.91	6.00	6.20
EABS	0.125	0.156	0.219	0.104	0.102	0.108	0.140	0.192	0.103	0.103	0.117	0.144	0.2060	0.107	0.098
SNE	**3.40**	3.52	4.53	3.61	3.82	**3.43**	3.56	4.55	3.61	3.80	**3.48**	3.551	4.61	3.50	3.77
Elovich equation															
α	0.131	0.135	0.144	0.155	0.152	0.134	0.135	0.139	0.133	0.133	0.159	0.154	0.1575	0.149	0.139
β	31.17	31.55	32.43	32.52	32.05	28.97	29.13	29.53	29.14	29.13	26.00	25.83	26.1119	25.38	25.02
ERRSQ	0.001	0.001	0.001	0.001	0.001	0.001	0.001	0.001	0.001	0.001	0.001	0.001	0.0010	0.001	0.001
HYBRID	0.035	0.035	0.036	0.039	0.040	0.033	0.033	0.033	0.033	0.033	0.037	0.036	0.0368	0.037	0.040
MPSD	5.97	5.83	5.70	6.02	6.18	5.49	5.46	5.42	5.47	5.47	5.12	5.10	5.08	5.24	5.62
ARE	4.51	4.47	4.44	4.29	4.31	4.19	4.17	4.16	4.14	4.14	4.22	4.22	4.23	4.20	4.18
EABS	0.094	0.096	0.099	0.096	0.094	0.098	0.097	0.097	0.097	0.097	0.117	0.117	0.1176	0.115	0.116
SNE	4.68	**4.67**	4.82	4.85	4.90	4.96	**4.94**	4.97	4.95	4.95	4.74	**4.74**	4.77	4.80	4.97
Intraparticle diffusion															
k	0.021	0.022	0.024	0.027	0.024	0.022	0.023	0.026	0.030	0.026	0.025	0.027	0.0291	0.033	0.028
ERRSQ	0.035	0.037	0.044	0.064	0.042	0.042	0.043	0.052	0.084	0.051	0.054	0.056	0.0666	0.100	0.061
HYBRID	1.70	1.65	1.76	2.26	1.73	1.86	1.81	1.93	2.71	1.92	2.12	2.06	2.20	2.91	2.12
MPSD	39.21	37.67	36.73	38.22	36.78	39.36	37.89	36.98	39.53	36.99	39.50	38.03	37.1225	39.01	37.25
ARE	33.14	32.04	30.54	29.63	30.69	33.67	32.64	31.04	29.90	31.06	33.54	32.49	31.2220	30.27	31.47
EABS	0.734	0.730	0.730	0.764	0.725	0.804	0.801	0.796	0.843	0.795	0.901	0.896	0.9033	0.948	0.891
SNE	4.26	**4.18**	4.29	4.87	4.23	4.13	**4.06**	4.13	4.89	4.12	4.22	**4.14**	4.25	4.89	4.16

Table 2
Isotherm constants with error analysis, at different pH values

	pH														
	4					5					6				
	ERRSQ	HYBRID	MPSD	ARE	EABS	ERRSQ	HYBRID	MPSD	ARE	EABS	ERRSQ	HYBRID	MPSD	ARE	EABS
Langmuir isotherm															
q_{max}	0.368	0.358	0.338	0.357	0.366	0.380	0.372	0.361	0.358	0.376	0.403	0.406	0.408	0.411	0.407
b	3.53	3.89	4.60	4.17	3.71	5.60	6.17	6.80	6.73	5.55	6.47	6.10	5.69	5.42	5.97
ERRSQ	0.004	0.005	0.006	0.005	0.004	0.003	0.003	0.004	0.004	0.003	0.007	0.007	0.008	0.008	0.007
HYBRID	0.161	0.157	0.182	0.167	0.160	0.118	0.108	0.118	0.120	0.124	0.355	0.349	0.358	0.373	0.349
MPSD	13.40	12.21	11.40	11.77	12.64	10.85	9.58	9.18	9.23	11.25	21.92	21.44	21.23	21.31	21.34
ARE	8.33	7.88	8.31	7.54	7.95	6.84	6.51	6.49	6.35	6.85	11.96	11.80	11.71	11.68	11.75
EABS	0.227	0.230	0.296	0.230	0.222	0.207	0.219	0.242	0.239	0.205	0.274	0.270	0.273	0.276	0.269
SNE	4.32	**4.18**	4.85	4.24	4.19	4.43	**4.30**	4.66	4.70	4.53	4.78	**4.73**	4.82	4.94	4.73
Freundlich isotherm															
k_F	0.257	0.253	0.254	0.269	0.253	0.291	0.290	0.293	0.294	0.294	0.317	0.313	0.311	0.322	0.313
n	2.92	2.58	2.28	2.16	2.90	3.20	2.79	2.38	2.54	3.41	3.38	2.83	2.44	2.76	3.62
ERRSQ	0.014	0.016	0.024	0.036	0.014	0.014	0.018	0.033	0.025	0.015	0.026	0.033	0.051	0.036	0.027
HYBRID	0.530	0.418	0.523	0.710	0.506	0.668	0.521	0.722	0.594	0.860	1.233	0.931	1.135	0.952	1.430
MPSD	28.90	20.02	16.61	17.52	27.60	35.83	25.66	20.70	21.60	42.24	42.55	28.87	24.54	28.70	47.20
ARE	16.50	14.38	13.44	13.17	15.89	18.11	15.30	15.38	13.88	19.75	23.64	19.96	20.46	19.85	25.04
EABS	0.452	0.488	0.558	0.586	0.445	0.475	0.523	0.651	0.571	0.458	0.643	0.723	0.879	0.735	0.629
SNE	3.89	**3.42**	3.73	4.40	3.76	3.71	**3.34**	4.10	3.56	4.17	3.95	**3.53**	4.13	3.60	4.25
Sips isotherm															
q_{max}	0.405	0.416	0.427	0.420	0.408	0.418	0.413	0.399	0.400	0.422	0.424	0.424	0.498	0.480	0.423
b	2.26	2.01	1.84	1.94	2.11	3.12	3.31	3.90	4.03	2.82	4.43	4.47	2.18	2.55	4.46
n	1.21	1.26	1.30	1.28	1.25	1.25	1.22	1.15	1.10	1.31	1.15	1.10	1.33	1.37	1.19
ERRSQ	0.003	0.003	0.003	0.003	0.003	0.001	0.001	0.001	0.002	0.001	0.006	0.007	0.012	0.008	0.007
HYBRID	0.104	0.102	0.104	0.103	0.103	0.066	0.065	0.069	0.094	0.072	0.383	0.358	0.441	0.424	0.461
MPSD	8.36	8.12	8.06	8.08	8.16	8.81	8.42	8.06	9.42	10.04	22.26	20.87	19.86	22.65	24.84
ARE	5.68	5.38	5.36	5.30	5.33	5.38	5.37	5.47	5.35	5.38	11.24	11.48	13.61	11.29	11.46
EABS	0.199	0.196	0.200	0.196	0.193	0.153	0.154	0.167	0.165	0.147	0.251	0.268	0.425	0.297	0.244
SNE	4.93	**4.83**	4.905	4.83	4.84	4.21	**4.18**	4.36	4.90	4.39	3.68	**3.67**	4.75	4.02	3.99
Redlich–Peterson isotherm															
k_R	1.60	1.87	2.16	2.10	1.63	2.91	2.97	2.91	2.58	2.68	3.28	2.58	2.48	2.69	2.91
a_R	4.69	5.79	7.01	6.76	4.89	8.28	8.50	8.30	7.21	7.52	8.54	6.42	6.18	6.78	7.40
β	0.92	0.87	0.82	0.82	0.91	0.90	0.89	0.89	0.91	0.91	0.91	0.98	0.95	0.97	0.96
ERRSQ	0.004	0.004	0.0049	0.004	0.004	0.001	0.001	0.001	0.001	0.001	0.007	0.007	0.008	0.007	0.006
HYBRID	0.129	0.120	0.1293	0.127	0.127	0.062	0.061	0.062	0.074	0.068	0.407	0.367	0.386	0.370	0.387
MPSD	10.50	9.13	8.73	8.75	10.26	7.76	7.77	7.73	8.50	8.08	23.04	21.46	21.17	21.77	22.64
ARE	6.83	6.46	6.31	6.25	6.64	4.93	4.97	4.98	4.89	4.90	12.16	11.77	12.15	11.77	11.80
EABS	0.221	0.226	0.241	0.238	0.218	0.137	0.139	0.141	0.138	0.138	0.300	0.271	0.309	0.269	0.265
SNE	4.70	**4.51**	4.75	4.69	4.64	**4.58**	4.60	4.62	4.96	4.76	4.86	4.53	4.86	**4.52**	4.58

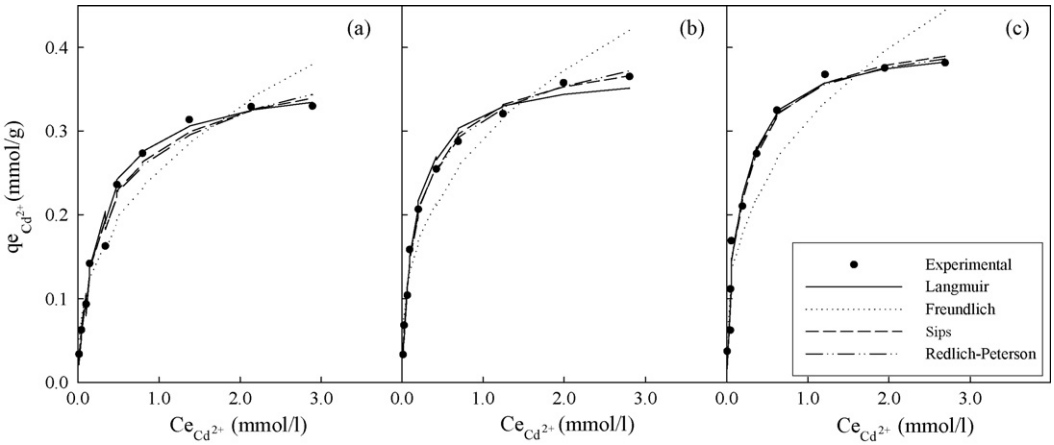

Fig. 6. Sorption isotherms of cadmium at (a) pH 4, (b) pH 5 and (c) pH 6.

Table 2 show the parameter sets obtained by fitting the experimental data to different models and using the corresponding error functions.

For 10 of the 12 cases studied (4 isotherm models × 3 pH values), HYBRID function provided the lowest SNE value (Table 2).

For the results presented in Fig. 6, the Langmuir, Sips and Redlich–Peterson isotherms provided accurate fits to the experimental data, while the Freundlich model showed the highest error values. This last equation predicts adsorption capacities lower than the experimental data at low liquid concentrations of cadmium, and higher than experimental values at high concentration of cadmium in solution.

The results obtained with the Langmuir isotherm show that an increase in pH within the range studied increased the maximum adsorption capacity and increased the value of the Langmuir constant. This indicates that the adsorption capacity and the affinity between the active sites and the metallic ions increase with increasing pH value. The q_{max} value is particularly useful in cases where the sorbent does not reach its full saturation as it enables the indirect comparison between different sorbates.

The Sips model provided slightly higher values of q_{max} than those obtained with the Langmuir model. The Sips model produced the best fitting isotherm parameters values for all the cases studied, and the lowest error values.

According to Sips model, the maximum adsorption capacity obtained for orange wastes was 0.40, 0.41 and 0.43 mmol/g at pH 4, 5 and 6, respectively. The magnitude of q_{max} was within the range of values obtained by several authors under similar conditions; for example: 0.22 mmol/g onto a natural polysaccharide [41], 0.48 mmol/g onto bone char [42], and 0.75 mmol/g onto *Ascophyllum nodosum* seaweed biomass [43].

The Redlich–Peterson isotherm shows that the value of β approaches unity, indicating that the Redlich–Peterson isotherm tends towards a Langmuir isotherm.

5. Conclusions

The results obtained in this study show that orange waste from the orange juice industry can be considered as a potential biosorbent material for the removal of Cd(II) ions from aqueous solutions. The FTIR spectra of the biosorbent before and after the adsorption shows that the adsorption capacity can be related to the carboxylic and the alcoholic hydroxyl groups of the orange waste.

Cadmium uptake is strongly affected by pH. When the pH was increased from 2 to 6, the percentage of cadmium uptake for a cadmium solution of 100 mg/l (0.89 mM) rose from 8 to 98%.

The adsorption kinetic is rapid and the equilibrium can be considered to be reached at 60 min, at pH values of 4–6. The Elovich equation is the best choice for describing the adsorption kinetic of cadmium ions onto orange waste since this material contains various types of binding site and therefore is a heterogeneous surface.

The equilibrium results have been modelled and evaluated using four different isotherm models at pH 4–6. The Sips model provided the best fit of the equilibrium data. According to this model, the maximum cadmium uptake was 0.40, 0.41 and 0.43 mmol/g at pH 4, 5 and 6, respectively.

It was demonstrated that the error function used to adjust the experimental data affects the parameter sets obtained. The HYBRID error function generally appears to produce the best fit for the models.

Acknowledgements

This work was financially supported by the Ministry of Science and Technology of Spain (REN2002-02030) and the European Regional Development Fund (ERDF). The authors gratefully acknowledge this economic support.

References

[1] G. Cimino, C. Caristi, Acute toxicity of heavy metals to aerobic digestion of waste cheese whey, Biol. Waste 33 (1990) 201–210.
[2] R. Salim, M.M. Al-Subu, E. Sahrhage, Uptake of cadmium from water by beech leaves, J. Environ. Sci. Health A27 (3) (1992) 603–627.
[3] C.W. Cheung, J.F. Porter, G. McKay, Elovich equation and modified second-order equation for adsorption of cadmium ions onto bone char, J. Chem. Technol. Biotechnol. 75 (2000) 963–970.

[4] J. De Zuane, Handbook of Drinking Water Quality Standards and Controls, Van Nostrand Reinhold, New York, 1990, pp. 64–69.
[5] C.W. Cheung, J.F. Porter, G. Mckay, Adsorption kinetic analysis for the removal of cadmium ions from effluents using bone char, Water Res. 35 (2001) 605–612.
[6] B. Volesky, Biosorption of Heavy Metals, CRC Press, Boston, USA, 1990, ISBN 0849349176, p. 408.
[7] M.C. Basso, E.G. Cerrella, A.L. Cukierman, Empleo de algas marinas para la biosorción de metales pesados de aguas contaminadas, Avances en Energías Renovables y Medio Ambiente 6 (2002), ISSN 0329-5184.
[8] S.H. Lee, C.H. Jung, H. Chung, M.Y. Lee, J.-W. Yang, Removal of heavy metals from aqueous solution by apple residues, Process. Biochem. 33 (1998) 205–211.
[9] S. Al-Asheh, F. Banat, R. Al-Omari, Z. Duvnjak, Predictions of binary adsorption isotherms for the adsorption of heavy metals by pine bark using single isotherm data, Chemosphere 41 (2000) 659–665.
[10] G. Cimino, A. Passerini, G. Toscano, Removal of toxic cations and Cr(VI) from aqueous solution by hazelnut shell, Water Res. 34 (2000) 2955–2962.
[11] G. Annadurai, R.-S. Juang, D.-J. Lee, Use of cellulose-based wastes for adsorption of dyes from aqueous solutions, J. Hazard. Mater. 92 (3) (2002) 263–274.
[12] F.A. Pavan, I.S. Lima, C. Airoldi, Y. Gushikem, Use of pokan Mandarin Peels as biosorbent for toxic metals uptake from aqueous solutions, J. Hazard. Mater 137 (2006) 527–533.
[13] K.K. Singh, R. Rastogi, S.H. Hasan, Removal of cadmium from wastewater using agricultural waste "rice polish", J. Hazard. Mater. A121 (2005) 51–58.
[14] A. Özcan, A.S. Özcan, S. Tunali, T. Akar, I. Kiran, Determination of the equilibrium, kinetic and thermodynamic parameters of adsorption of copper(II) ions onto seeds of *Capsicum annuum*, J. Hazard. Mater. B124 (2005) 200–208.
[15] M. Madhava Rao, A. Ramesh, G. Purna Chandra Rao, K. Seshaiah, Removal of copper and cadmium from the aqueous solutions by activated carbon derived from *Ceiba pentandra* hulls, J. Hazard. Mater. B129 (2006) 123–129.
[16] K.N. Ghimire, K. Inoue, H. Yamaguchi, K. Makino, T. Miyajima, Adsorptive separation of arsenate and arsenite anions from aqueous medium by using orange waste, Water Res. 37 (2003) 4945–4953.
[17] Y.S. Ho, G. McKay, The kinetic of adsorption of divalent metal ions onto sphagnum moss peat, Water Res. 34 (2000) 735–742.
[18] S. Lagergren, Zur theorie der sogenanten adadsorption gelöster stoffe, Kungliga Svenska Vetenskapsakademiens, Handlingan Band. 24 (1898) 1–39 (cited in [23]).
[19] Y.S. Ho, G. McKay, A comparison of chemisorption kinetic models applied to pollutant removal on various sorbents, Inst. Chem. Eng. 76 (1998) 332–340.
[20] M.X. Loukidou, A.I. Zouboulis, T.D. Karapantsios, K.A. Matis, Equilibrium and kinetic modelling of chromium (VI) biosorption by *Aeromonas caviae*, Colloid Surf. A 242 (2004) 93–104.
[21] M. Özacar, I.A. Sengil, A kinetic study of metal complex dye adsorption onto pine sawdust, Process Biochem. 40 (2005) 565–572.
[22] E. Fourest, C.J. Roux, Heavy metal biosorption by fungal mycilial by-products: mechanisms and influence of pH, Appl. Microbiol. Biotechnol. 37 (1992) 399–403.
[23] I. Langmuir, The adsorption of gases on plane surfaces of glass, mica and platinium, J. Am. Chem. Soc. 40 (1918) 1361–1403 (cited in [23]).
[24] H. Freundlich, Uber die adsorption in Losungen. Zeitschrift für Physikalische, CEIME 57 (1907) 385–470 (cited in [23]).
[25] R. Sips, On the structure of a catalyst surface, J. Chem. Phys. 16 (5) (1948) 490–495 (cited in [23]).
[26] O. Redlich, D.L. Peterson, A useful adsorption isotherm, J. Phys. Chem. 63 (1959) 1024–1026 (cited in [23]).
[27] Y.S. Ho, J.F. Porter, G. McKay, Equilibrium isotherm studies for the adsorption of divalent metal ions onto peat: copper, nickel and lead single components systems, Water Air Soil Poll. 141 (2002) 1–33.
[28] J.F. Porter, G. McKay, K.H. Choy, The prediction of adsorption from binary mixture of acidic dyes using single- and mixed-isotherm variants of the ideal adsorbed solute theory, Chem. Eng. Sci. 54 (1999) 5863–5885.
[29] D.W. Marquardt, An algorithm for least-squares estimation of nonlinear parameters, J. Soc. Ind. Appl. Math. 11 (1963) 431–441.
[30] A. Kapoor, R.T. Yang, Correlation of equilibrium adsorption data of condensable vapours on porous adsorbents, Gas Sep. Purif. 3 (4) (1989) 187–192.
[31] F. Pagnanelli, M.P. Petrangeli, L. Toro, M. Trifoni, F. Veglio, Biosorption of metal ions on *Arthrobacter* sp.: biomass characterization and biosorption modelling, Environ. Sci. Technol. 34 (2000) 2773–2778.
[32] P. Brown, S. Gill, S.J. Allen, Determination of optimal peat type to potentially capture copper and cadmium from solution, Water Environ. Res. 73 (3) (2001) 351–362.
[33] L. Norton, K. Baskaran, T. McKenzie, Biosorption of zinc from aqueous solutions using biosolids, Adv. Environ. Res. 8 (2004) 629–635.
[34] M. Ajmal, A.H. Khan, S. Ahamd, A. Ahmad, Role of sawdust in the removal of copper (II) from industrial wastes, Water Res. 32 (10) (1998) 3085–3091.
[35] M. Ajmal, R.A.K. Rao, R. Ahmad, J. Ahmad, Adsorption studies on *Citrus reticulata*: removal and recovery of Ni(II) from electroplating wastewater, J. Hazard. Mater. B79 (2000) 117–131.
[36] Y. Nuhoglu, E. Oguz, Removal of copper(II) from aqueous solutions by biosorption on the cone biomass of *Thuja orientalis*, Process Biochem. 38 (2003) 1627–1631.
[37] C.F. Baes, R.E. Mesmer, The Hydrolysis of Cations, Krieger Publishing Company Malabar, Florida, 1986.
[38] W. Ma, J.M. Tobin, Determination and modelling of effects of pH on peat biosorption of chromium, copper and cadmium, Biochem. Eng. J. 18 (2004) 33–40.
[39] D. Kratochvil, B. Volesky, Advances in the biosorption of heavy metals, Trends Biotechnol. 16 (1998) 291–300.
[40] H. Teng, C. Hsieh, Activation energy for oxygen chemisorption on carbon at low temperatures, Ind. Eng. Chem. Res. 38 (1999) 292–297.
[41] Z. Reddad, C. Gérente, Y. Andrès, M.C. Ralet, J.F. Thibault, P. Le Cloirec, Ni(II) and Cu(II) binding properties of native and modified sugar beet pulp, Carbohyd. Polym. 49 (1) (2002) 23–31.
[42] D.C. Ko, C.W. Cheung, K.K.H. Choy, J.F. Porter, G. McKay, Adsorption equilibria of metal ions on bone char, Chemosphere 54 (2004) 273–281.
[43] K.-H. Chong, B. Volesky, Description of two-metal biosorption equilibria by Langmuir-type models, Biotechnol. Bioeng. 47 (1995) 451–460.